MICRO TECHNOLOGY IN HEAT PUMPING SYSTEMS[1]

S.T. MUNKEJORD, H.S. MÆHLUM, G.R. ZAKERI[§], P. NEKSÅ[†], J. PETTERSEN[*‡]

SINTEF Energy Research, Refrigeration and Air Conditioning
Kolbjørn Hejes vei 1D, N-7465 Trondheim, Norway
Contact e-mail: svend.t.munkejord@energy.sintef.no

[*]Norwegian University of Science and Technology NTNU, Refrigeration and Air Conditioning, Norway

[†] Vice-president, IIR Commission E2
[‡] Member of IIR, Commission B2
[§] Associate member of IIR

Key words: Microscale heat pumps, micro heat exchangers, heat transfer, pressure drop, condensation

ABSTRACT

Micro heat pumps, with dimensions in the order of centimetres, may in the future be utilised for the heating and/or cooling of buildings, vehicles, clothing, and other products or applications. A number of issues have yet to be solved, including the construction of a microscale compressor, and determination of micro heat exchanger heat transfer capacities.

Test samples of micro heat exchangers and a corresponding test apparatus have been built. Some two-phase experiments with propane (R-290) as refrigerant have been conducted. Preliminary results for a micro condenser with 0.5 mm wide trapezoidal channels of 25 mm length showed that a heat flux of up to 135 kW/m², based on the refrigerant-side area, was attainable. The corresponding overall heat transfer coefficient was 10 kW/(m²K), with a refrigerant mass flux of 165 kg/(m^{2}s) and a refrigerant-side pressure drop of 180 kPa/m.

1. INTRODUCTION

In the micro electro-mechanical systems (MEMS) technology, the production techniques of computer chips is being applied to produce mechanical structures. For example, heat exchangers may be produced by etching channels in silicon. Such heat exchangers may have a channel width in the order of 0.1 mm (= 100 μm), with a channel length of a few centimetres.

There are several motivations for developing microscale heat pumping systems. First, the heat transfer and pressure drop characteristics of flow in microchannels are favourable. This may, somewhat simplified, be seen from the definition of the heat transfer coefficient, $\alpha = C\,\lambda\,/d$, where C is usually regarded as a constant in laminar flow. The smaller the characteristic dimension d, the better the heat transfer coefficient.

Second, the interconnection of several micro heat pumping units makes a stepwise approximation to theoretical cycles possible, thus improving system efficiency.

Next, small heat pumping units allow distributed heating/cooling and good regulation. This reduces ducting and cycling losses, as stated by Drost, Beckette and Wegeng[1].

Finally, using the same production techniques as for integrated circuits, economies of production seem realisable[2]. Therefore the use of MEMS technology for heat pumping applications seems promising.

Possible applications of microscale heat pumps could be space heating or cooling in vehicles or buildings, microprocessor cooling, and portable cooling devices. Furthermore, one could imagine micro heat pumps being integrated in products as diverse as prefabricated wall elements, or in suits for use in extreme climatic conditions.

---

[1] This is a slightly edited and extended version of a paper originally presented at the 20th International Congress of Refrigeration, IIR/IIF, Sydney, 1999

2. BASIC CONSIDERATIONS

It is our aim to produce a microscale heat pump operating with a vapour compression cycle. Three basic types of items are required to make such a heat pump: Heat exchangers, a compressor, and a throttling device. A compressor is currently not available. The throttling device could simply be some sort of micro capillary tube. So far, we have concentrated on the heat exchangers. To be able to dimension a micro scale heat pump, it is necessary to know the heat transfer capacity of the heat exchangers.

2.1 Heat transfer

Since the pioneering effort by Tuckerman and Pease[3] on the cooling of very large-scale integrated circuits (VLSI), a great deal of work has been conducted on single-phase heat transfer in microchannels. However, the present authors are only aware of a limited number of publications, and no heat transfer correlations, on evaporation and condensation. Such data are important to dimension and assess the usefulness of microscale heat pumps.

A channel dimension of micrometres is in the same order of magnitude as the thermal and hydrodynamic boundary layers. This leads to molecular effects becoming significant. The theory on forced convection inside microchannels is a developing area.

In their review of single-phase forced convection heat transfer in microgeometries, Bailey, Ameel, et al.[4] summarised the following effects which are normally neglected when considering macroscale flow, but which may exist in microscale convection:

- Both momentum and heat transfer in other directions than the streamwise direction can increase significantly.
- Temperature variations of the transport fluid can cause a significant variation in fluid properties throughout a microsystem, invalidating the often-used assumption of constant properties.
- In liquids, the influence of molecular polar forces increases.
- Changes in the apparent fluid viscosity have been observed.

Besides these effects, some conditions can exist in microscale flow that are not normally seen in macroscale flow, such as slip flow.

These factors can affect the shape of velocity and temperature profiles to the extent that heat and momentum transport are no longer of the same order of magnitude. Thus, the Reynolds analogy is no longer valid, as has been found by several researchers[4].

Turbulent heat transfer is apparently higher than theory predicts. For example, the following single-phase correlation was found by Wu and Little[5] for different flat channels with a hydraulic diameter of about 150 μm:

$$\mathrm{Nu} = 0.00222\,\mathrm{Pr}^{0.4}\,\mathrm{Re}^{1.09}\text{, where Re} > 3{,}000 \tag{1}$$

It should be noted that the relative roughness of the microchannels was high.

Choi, Barron and Warrington[6] measured convective heat transfer coefficients for cooling of nitrogen in microtubes whose inside diameters ranged from 3 to 81 μm. For laminar flow, Re < 2,000, they found

$$\mathrm{Nu} = 0.000972\,\mathrm{Re}^{1.17}\,\mathrm{Pr}^{1/3} \tag{2}$$

which is in disagreement with the notion that the laminar Nusselt number is a constant, which applies to fully developed macroscale flow. For turbulent flow, 2,500 < Re < 20,000, they found

$$\mathrm{Nu} = 3.82\cdot 10^{-6}\,\mathrm{Re}^{1.96}\,\mathrm{Pr}^{1/3} \tag{3}$$

which is as much as seven times higher than that predicted by the Dittus-Boelter equation, which was developed for turbulent flow in smooth macro tubes.

The results cited above are for single-phase flow, mostly for cooling of electronic equipment, where temperature differences and heat fluxes are greater than they would be in a heat pumping application. Therefore, for instance varying fluid properties are not likely to be that important in our case. Nevertheless, it seems clear that the common macroscale heat transfer correlations cannot be used when dimensioning microscale heat pumps.

2.2 Pressure drop

Friction factors in laminar microchannel flow are apparently lower than macroscale predictions. Choi, Barron and Warrington[6] found that the product of the friction factor and the Reynolds number, $f \cdot \mathrm{Re}$, yielded a value of 53 for laminar flow in microtubes having inside diameters smaller than 10 μm, in contrast to the classical 64. In the turbulent region, their data could be correlated by the expression

$$f = 0.140\,\mathrm{Re}^{-0.182} \tag{4}$$

which predicts friction factors 10 % to 30 % lower than those predicted by the Blasius relation.

For two-phase flow, few results pertaining to heat transfer and pressure drop are available.

2.3 Compressor

There are several possibilities for construction of a microscale compressor. A number of fundamental principles are available for converting electric power into mechanical displacement or forces that can create displacement:

- piezolectric effect
- electrodynamic effect
- electrostatic effect

Displacement may also be achieved through various thermal actuators, for instance based on:

- shape memory alloy subjected to varying temperature
- gas/liquid phase change
- thermal expansion/contraction of a gas (thermopneumatic actuation)
- solid material combinations with different thermal expansion coefficient

Piezoelectric pumps or compressors with membrane displacement have been built from bimorph materials (two bonded layers that bend when subjected to voltage)[7], and from piezoelectric elements bonded to flexible membranes[8]. These designs are able to amplify the small displacement of piezoelectric materials. A general problem in membrane compressors is the large clearance volume. Losses due to hysteresis in the piezoelectric material must also be considered. Some of the other principles mentioned above may have problems in achieving sufficient compression pressure and speed of operation. Thermal actuators improve their dynamic response as size is reduced, however.

It is also possible to conceive miniaturized conventional rotating compressors. Epstein, Senturia et al.[9] is reporting development of a microscale (10 mm by 3 mm) gas turbine generator. This may ultimately lead to the development of a motor-driven turbocompressor. Hitachi[10] has developed a trochoid micropump of 7 mm diameter that is able to handle pressures at 1 MPa, a design that may be converted into a compressor.

Since microscale pumps are available, one might imagine that the first microscale heat pumps use an absorption process that avoids compressor requirements. Drost and Friedrich[11] reported the development of such a heat pump, although it will be “mini” rather than “micro”, with dimensions of 90 mm × 90 mm × 60 mm.

3. TEST APPARATUS

A test apparatus for testing micro heat exchangers has been built at SINTEF Energy Research. The purpose of the test programme is to obtain knowledge about two-phase heat transfer in micro heat exchangers, as well as to gain experience with MEMS technology in general. This is regarded as a first step in determining whether a vapour compression heat pumping system based on MEMS technology might be feasible.

The channels of the micro heat exchangers were made in silicon. The thermal conductivity and the density of silicon are comparable to those of aluminium, whereas the tensile strength is better than that of steel, and the thermal expansion coefficient is one fourth of that of steel.

The heat exchanger channels were made using a photolithographic etching technique. A mask was applied on the silicon wafer, after which the desired shapes could be etched. TMAH (tetramethyl ammonium hydroxide) was used as etchant. The channels were sealed off by attaching pyrex plates by anodic bonding. For the condenser, channels were etched into the silicon substrate on both sides. A 1.2 μm thick aluminium resistance film was sputtered onto the reverse side of the evaporator to provide the necessary heat. Details of the condenser are shown in Figure 1. The evaporator was identical to the condenser, except that channels were etched only on one side of the silicon substrate. The angle of 144.7° is due to the properties of silicon.

Three separate heat exchanger types (A, B, C) were etched onto each circular silicon wafer of 100 mm diameter. Thus different channel cross sections could relatively conveniently be tested. The channel dimensions are given in Table 1. The same channel sizes occured in both the condenser and the evaporator. The water channels, however, had w_{ct} = 500 μm for each of the three condensers. Note that the A and B channel cross-sections are triangular.

The condensers are shown on the photograph in Figure 2. The three heat exchangers were located on the small disc in the middle. Each individual condenser had its own refrigerant and water connections, and the refrigerant and water tubes were connected according to which condenser was to be tested.

A schematic overview of the test apparatus is given in Figure 3. The aim with the test apparatus was to simulate an actual heat pumping process. Therefore, it consisted of a condenser (1), a throttle valve (9) and an evaporator (2). Since a compressor was not available, an open circuit was used. The heat exchangers were mounted horizontally.

Slightly superheated refrigerant entered the condenser, where it was condensed against the cool water in a counter-flow configuration. The refrigerant inlet condition at the condenser was controlled with a throttle valve (5), a pre-heater (6), as well as electrical heating of the refrigerant bottle (4). The city water used in the refrigerant pre-heater had an initial temperature of about 7 °C, and it was heated to the desired inlet temperature with an electrical thermostat-controlled heater. The same was valid for the water that flowed through the condenser. After the expansion valve, the refrigerant (propane) entered the electrically heated evaporator, after which it was released into the atmosphere.

4. DATA ACQUISITION AND REDUCTION

Data were read on a digital voltmeter and evaluated in a spreadsheet. Readings were taken over an interval of about 10 minutes for each data point. Temperatures were measured with calibrated type E thermocouples of 0.07 mm diameter. The standard uncertainty in the temperature measurements was estimated to be ± 0.08 K. The standard uncertainty of the differential pressure measurements, with a range of range 0–100 kPa was ± 0.05 % of the reading, whereas the standard uncertainty of the absolute pressure measurement, with a range of 100–1600 kPa, was ± 0.1 % of the reading. The mass flow rates were measured using

scales and a stopwatch. For the refrigerant scale, the standard uncertainty was ± 1 g, and for the water it was ± 0.1 g. The uncertainty in the stopwatch reading was assumed to be ± 0.15 s. The power dissipated in the evaporator heating film was found by measuring the voltage across a precision resistance, as well as the voltage across the heating film.

The overall heat transfer coefficient (W/m^{2}K) by condensation was calculated as follows:

$$k = \frac{\dot{Q}}{A_{ref}\Delta T_{lm}} \tag{5}$$

where $\dot{Q}$ (W) is the heat flow rate absorbed on the water side, A_{ref} is the refrigerant-side heat transfer area, and the logarithmic mean temperature difference ΔT_{lm} (K) was calculated by

$$\Delta T_{lm} = \frac{\Delta T_1 - \Delta T_2}{\ln \dfrac{\Delta T_1}{\Delta T_2}} \tag{6}$$

where $\Delta T_1 = T_{\mathrm{sat,ref}}(p_o) - T_{\mathrm{H2O},o}$ and $\Delta T_2 = T_{\mathrm{sat,ref}}(p_i) - T_{\mathrm{H2O},i.}$ This definition of the temperature differences ΔT_1 and ΔT_2 may only be applied for condensation when the inlet superheating and outlet subcooling is "low". The standard uncertainty in the overall heat transfer coefficient k was estimated to be in the range of 4 %. (Therefore, the uncertainty was around 8 % at a 95 % confidence level).

The heat flux for the condenser and the evaporator was calculated as follows:

$$\dot{q} = \frac{\dot{Q}}{A_{ref}} \tag{7}$$

where $\dot{Q}$ and A_{ref} are explained above. The above equations may also be used for evaporation, except that the heat flow rate is then calculated from the dissipated heat in the resistance heater. For the evaporator tests, the heat transfer coefficient could be calculated directly:

$$\alpha = \frac{\dot{Q}}{A_{ref}\Delta T_{lm}} \tag{8}$$

where now $\Delta T_1 = T_w - T_{\mathrm{sat,ref}}(p_o)$ and $\Delta T_2 = T_w - T_{\mathrm{sat,ref}}(p_i)$ were inserted into the definition of ΔT_{lm}. The wall temperature T_w was calculated by measuring the temperature on the reverse side of the silicon wafer, and assuming one-dimensional heat transfer through the wafer. The wall temperature was assumed constant in the heat exchanger.

5. EXPERIMENTAL RESULTS

Tests with propane (R-290) as a refrigerant have been conducted. Presently, only preliminary results are available, and unfortunately, no data for heat exchanger A have been obtained thus far.

Figure 4 shows the measured overall heat transfer coefficient k during condensation in heat exchanger C (refer to Table 1 for details) as a function of varying refrigerant mass flux. The tests were run with a constant water mass flux of (1860^{+46}_{-75}) kg/(m^{2}s). The water inlet temperature was varied from 17.0 °C to 24.5 °C. Then the refrigerant mass flow rate was varied in such a way that full condensation took place. The corresponding mass fluxes ranged from 56.2 kg/(m^{2}s) to 122.6 kg/(m^{2}s). The refrigerant inlet state was typically about 1 K superheated, and the exit was around 6 K subcooled. It could be observed through the glass cover of the condenser that about 1/5 of the condenser length was filled with liquid at the exit.

Tests were conducted with two different condensation temperatures, 32 °C and 39 °C. The measured overall heat transfer coefficients k ranged from 8350 W/(m^{2}K) to 7090 W/(m^{2}K), with a decreasing trend for increasing refrigerant mass fluxes. The condensation heat transfer rates lay between 20.6 W and 48.5 W, giving heat fluxes from 51.7 kW/m^2 to 121.5 kW/m^2. The refrigerant-side pressure drop varied from 1.3 kPa to 2.5 kPa, as can be seen in Figure 6.

Additional tests with heat exchanger C and higher mass fluxes showed that a heat flux $\dot{q}$ of 135 kW/m^2 was attainable, with a mean logarithmic temperature difference of ΔT_{lm} = 13 K. The corresponding overall heat transfer coefficient k was 10 kW/(m^{2}K), with a refrigerant-side pressure drop of 4.5 kPa (180 kPa/m). The condensation temperature was 36 °C, whereas the refrigerant and water mass fluxes were 165 kg/(m^{2}s) and 3000 kg/(m^{2}s), respectively. The measured refrigerant-side pressure drop corresponded to 0.15 K drop in saturation temperature.

Measurements of the overall heat transfer coefficient k during condensation in heat exchanger B as a function of varying refrigerant mass flux are shown in Figure 5. The test procedure was the same as the one described for heat exchanger C, and the refrigerant-side mass fluxes varied from 32.3 kg/(m^{2}s) to 145.0 kg/(m^{2}s). Due to limitations in the test apparatus, the water mass flux could only be kept within (2100^{+52}_{-121}) kg/(m^{2}s). The water inlet temperature was varied from 17.0 °C to 24.4 °C. Three test series were made; one with 25 °C, one with 33 °C, and another with 39 °C condensation temperature. The measured overall heat transfer coefficients k lay between 8520 W/(m^{2}K) and 6980 W/(m^{2}K), again with a slightly decreasing trend for increasing refrigerant mass flux. The condensation heat transfer rates ranged from 8.4 W to 36.6 W, corresponding to heat fluxes from 25.8 kW/m^2 to 112 kW/m^2. The refrigerant-side pressure drop, which ranged from 0.83 kPa to 2.3 kPa, is shown in Figure 7.

Initial evaporation tests have also been conducted. They showed that for conditions similar to the the condensation tests, heat transfer coefficients on the order of 20 kW/(m^{2}K) were easily obtainable.

6. CONCLUSIONS

- General conclusions as to the heat transfer and pressure drop in heat exchangers of microscale heat pumps cannot be drawn on the basis of the somewhat scarce data yet available from this investigation. However, it seems clear that quite high heat fluxes and heat transfer coefficients are attainable at relatively low pressure drops. Further work and more experiments are needed.
- A microscale compressor is presently not available, although it seems that a microscale electrically driven microcompressor may be developed. Further work is needed also in this respect.
- The possibilities for applying microscale heat pumps for heating or cooling of devices, humans, and buildings, seem interesting, given that the required components can be realised.
- The greatest advantages foreseen for the microscale heat pump are economies of production, reduction of losses due to distribution, as well as high coefficients of performance due to good adaptation to ideal processes.

Acknowledgements: The tested heat exchangers were made at SINTEF Electronics and Cybernetics, Oslo, Norway. Hydro Aluminium provided partial funding for the project.

7. REFERENCES

1. M. K. Drost, M. R. Beckette and R. S. Wegeng, 1994, Thermodynamic Evaluation of a Microscale Heat Pump, Proceedings of the 1994 International Mechanical Engineering Congress and Exposition, ASME, p. 35-40.
2. T. A. Ameel, R. O. Warrington, R. S. Wegeng and M. K. Drost, 1997, Miniaturization technologies applied to energy systems, Energy Conversion and Management, vol. 38, no. 10-13: p. 969-982.
3. D. B. Tuckerman and R. F. W. Pease, 1981, High-Performance Heat Sinking for VLSI, IEEE Electronic Device Letters, vol. EDL-2, no. 5: p. 126-129.
4. D. K. Bailey, T. A. Ameel, J. Warrington, Robert O. and T. I. Savoie, 1995, Single Phase Forced Convection Heat Transfer in Microgeometries – a Review, Proceedings of the 1995 30th Intersociety Energy Conversion Engineering Conference, IECEC, ASME, p. 301-310.
5. P. Wu and W. A. Little, 1984, Measurement of the heat transfer characteristics of gas flow in fine channel heat exchangers used for microminiature refrigerators, Cryogenics, vol. 24: p. 415-420.
6. S. B. Choi, R. F. Barron and R. O. Warrington, 1991, Fluid Flow and Heat Transfer in Microtubes, Winter Annual Meeting of the American Society of Mechanical Engineers, ASME, p. 123-134.
7. T. Narasaki, 1978, The characteristics of bimorph vibrator pump, Proceedings of the 13th Intersociety Energy Conversion Engineering Conference, San Diego, vol. 2, p. 2005-2010.
8. K. Uchino, 1997, Piezoelectric Actuators and Ultrasonic Motors, Boston/Dordrecht/London, Kluwer Academic Press.
9. A. H. Epstein, S. D. Senturia, G. Anathasuresh, A. Ayon, K. Breuer, K.-S. Chen, F. E. Ehrich, G. Gauba, R. Ghodssi, C. Groshenry, S. Jacobson, J. H. Lang, C.-C. Lin, A. Mehra, J. O. Mur Miranda, S. Nagle, D. J. Orr, E. Piekos, M. A. Schmidt, G. Shirley, S. M. Spearing, C. S. Tan, Y.-S. Tzeng and I. A. Waitz, 1997, Power MEMS and microengines, Proceedings Proceedings of the 1997 International Conference on Solid-State Sensors and Actuators, Part 2, SPIE, p. 753-756.
10. Hitachi, 1996, Quarterly Magazine "Micromachine", vol. 14. Micromachine Center, Japan (http://202.232.157.4/MMC/no.14/act/26/hitach.htm).
11. M. K. Drost and M. Friedrich, 1997, Miniature heat pumps for portable and distributed space conditioning applications, Proceedings of the 1997 32nd Intersociety Energy Conversion Engineering Conference, Part 2, IEEE, p. 1271-1274.

NOMENCLATURE

A	Area, m^2
b	Total width, m
d_h	Hydraulic diameter, m
f	Darcy friction factor, m
k	Overall heat transfer coefficient, $W/(m^2K)$
l	Length, m
$\dot{m}$	Mass flux, $kg/(m^2s)$
N_{ch}	Number of channels
Nu	Nusselt number
p	Pressure, Pa
Pr	Prandtl number
$\dot{q}$	Heat flux, W/m^2
$\dot{Q}$	Heat transfer rate, W
Re	Reynolds number
T	Temperature, K
w	Width, m
α	Heat transfer coefficient, $W/(m^2K)$
Δ	Difference
λ	Thermal conductivity, W/(m K)

Subscripts:

c	Cross-section
cb	Channel bottom
ct	Channel top
lm	Logarithmic mean
i	Inlet
o	Outlet
ref	Refrigerant

FIGURES

Figure 1: Details of the micro condenser.
Figure 2: Close-up of condensers.
Figure 3: Schematics of test apparatus.
Figure 4: Overall heat transfer coefficient by condensation as a function of refrigerant mass flux for heat exchanger C
Figure 5: Overall heat transfer coefficient by condensation as a function of refrigerant mass flux for heat exchanger B
Figure 6: Refrigerant-side pressure drop by condensation as a function of mass flux in heat exchanger C
Figure 7: Refrigerant-side pressure drop by condensation as a function of mass flux in heat exchanger B

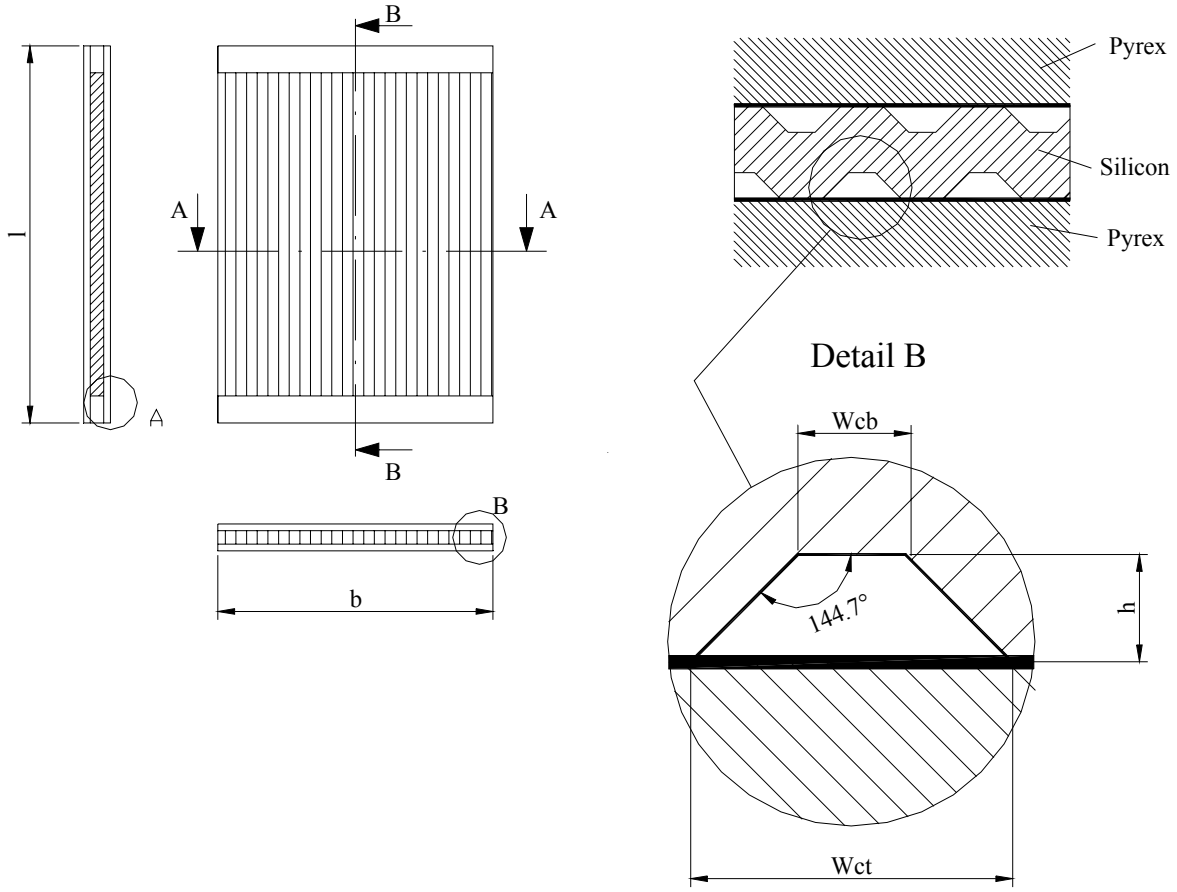

Figure 1: Details of the micro condenser.

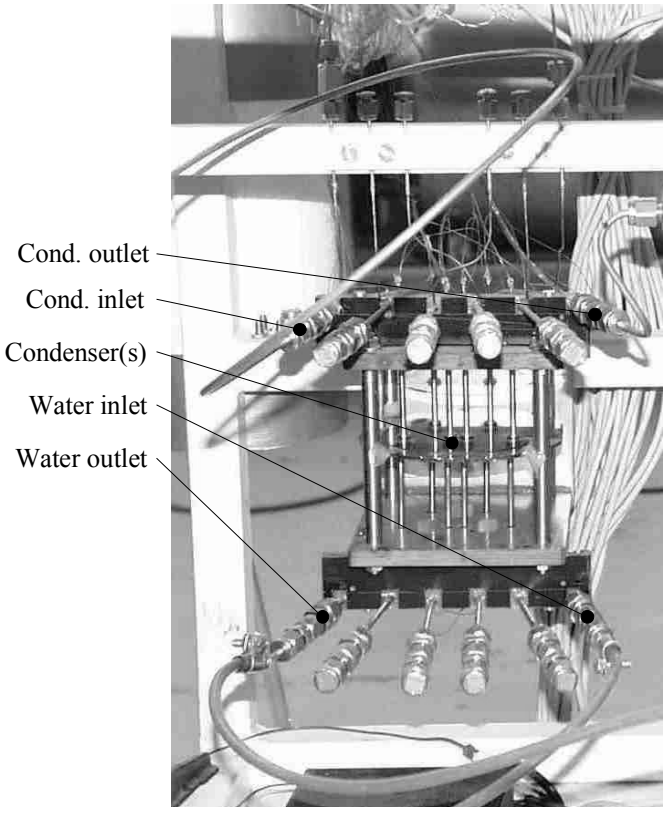

Figure 2: Close-up of condensers.

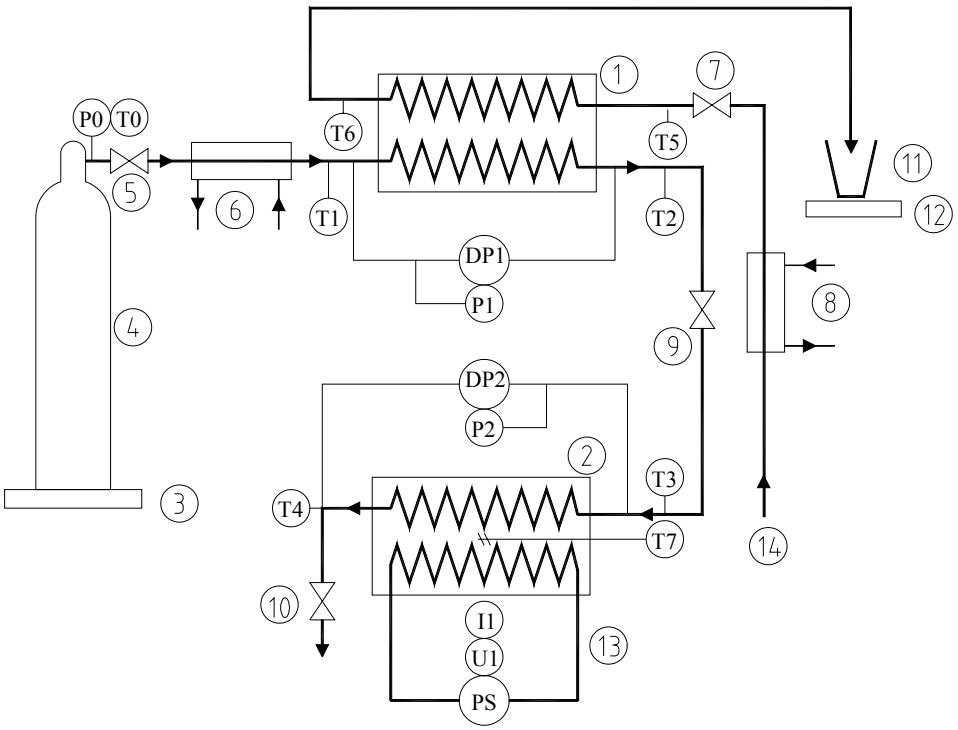

Figure 3: Schematics of test apparatus.

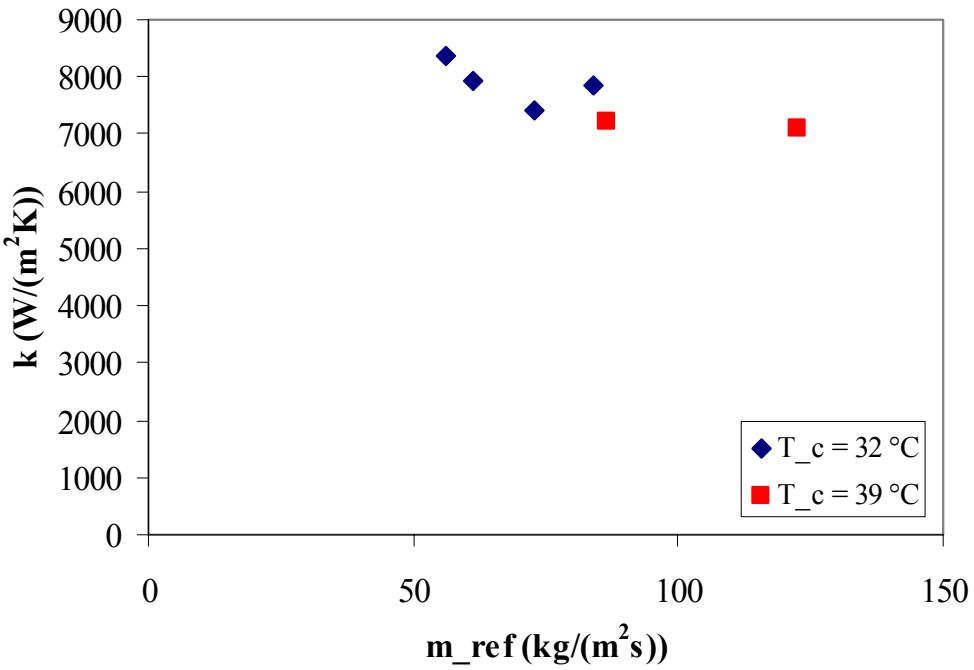

Figure 4: Overall heat transfer coefficient by condensation as a function of refrigerant mass flux for heat exchanger C.

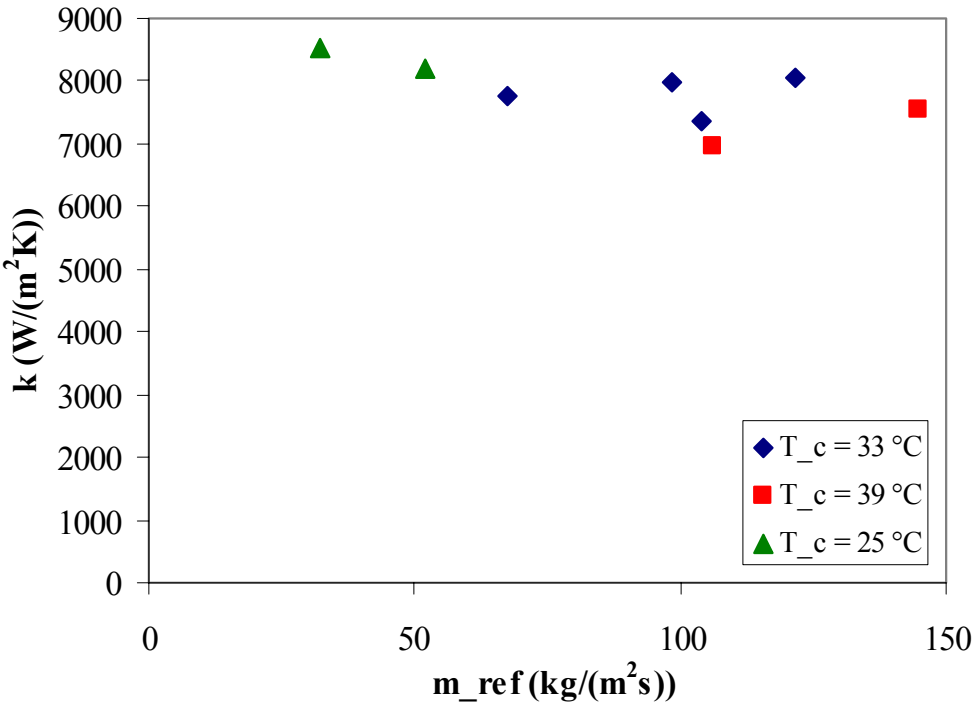

Figure 5: Overall heat transfer coefficient by condensation as a function of refrigerant mass flux for heat exchanger B.

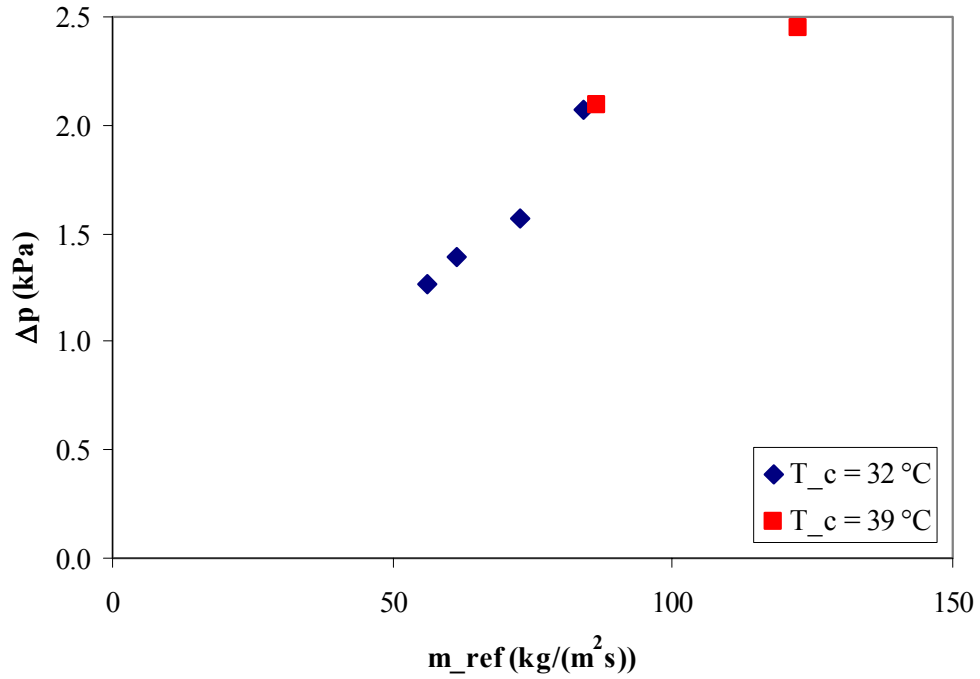

Figure 6: Refrigerant-side pressure drop by condensation as a function of mass flux in heat exchanger C.

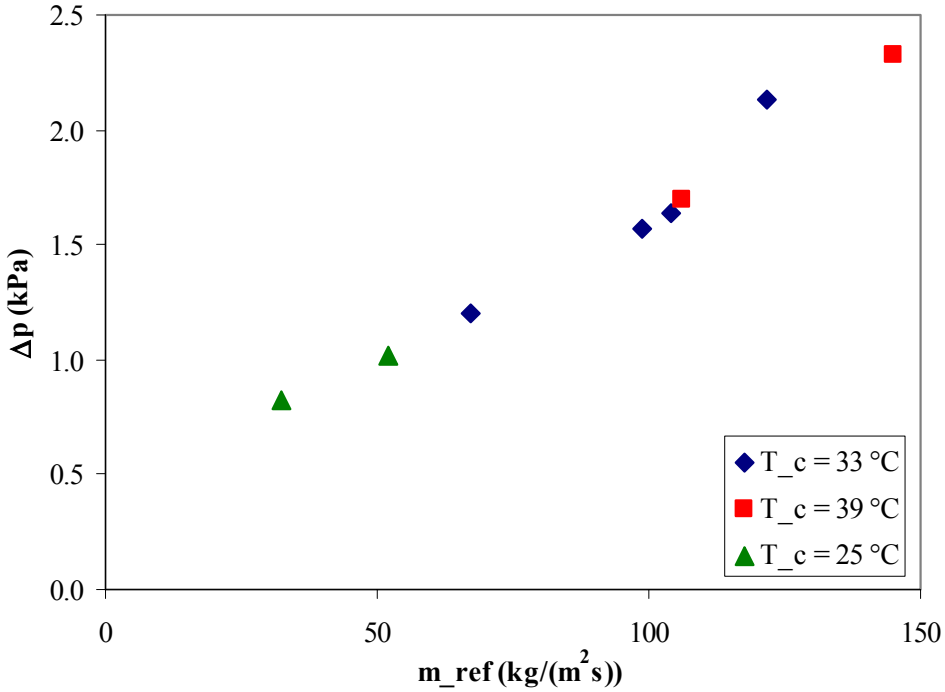

Figure 7: Refrigerant-side pressure drop by condensation as a function of mass flux in heat exchanger B.

Table 1: Dimensions of microchannel heat exchangers.

Type	Top width, w_{ct} (μm)	Channel height, h (μm)	Bottom width, w_{cb} (μm)	Hydraulic diameter d_h (μm)	No. of channels N_{ch} (–)	Tot. flow area A_c (10^{-6} m^2)	Refrig.-side area A_{ref} (10^{-4} m^2)	Length[1)] l (mm)	Width b (mm)
A	200	70.8	0.0	63.6	67	0.474	3.28	20	20
B	350	123.9	0.0	111.4	38	0.824	3.26	20	19.775
C	500	141.0	101.7	155.7	27	1.15	3.98	25	20

1) Length excluding headers (A, Figure 1), 2mm on each side.